Experimental Thermal and Fluid Science 85 (2017) 354–362

Contents lists available at ScienceDirect

Experimental Thermal and Fluid Science

journal homepage: www.elsevier.com/locate/etfs

Flow-induced vibration of a circular cylinder surrounded by two, four and eight wake-control cylinders

M. Silva-Ortega [1], G.R.S. Assi [*,2]

Department of Naval Architecture & Ocean Engineering, EPUSP University of São Paulo, São Paulo, SP, Brazil

ARTICLE INFO

Article history:
Received 24 October 2016
Received in revised form 13 March 2017
Accepted 13 March 2017
Available online 18 March 2017

Keywords:
Vortex-induced vibration
Galloping
Suppression
Wake control
Drag reduction

ABSTRACT

The present work investigates the use of a polar array of 2, 4 and 8 wake-control cylinders as a means to suppress the vortex-induced vibration (VIV) of a larger circular cylinder. The diameter of the control cylinders and the gap between their walls have been varied in 27 different configurations. Experiments have been performed in water at Reynolds numbers between 5000 and 50,000. Cross-flow amplitude of displacement, frequency of vibration, mean drag and fluctuating lift coefficients are presented. While some configurations of control cylinders suppressed VIV, others produced a galloping-like response. The best VIV suppressor was composed of 8 control cylinders and mitigated 99% of the peak amplitude of vibration when compared to that of a plain cylinder; mean drag was increased by 12%. A polar array of 4 control cylinders was the most efficient configuration to minimize the mean drag, but the system developed severe vibrations combining VIV and a galloping-like response. The system appeared to be very sensitive to the parameters investigated; small variations in the size and position of the control cylinders produced unexpected responses.

1. Introduction

The vortex-shedding mechanism of a circular cylinder can be controlled, at least in theory, by the interference of small wake-control cylinders positioned around the circumference of the main body. Strykowski and Sreenivasan [18] and others have showed that this strategy is possible for low Reynolds numbers. Such control cylinders interact with the boundary layer and/or the separated shear layers, disrupting the formation of vortices that are convected downstream to form a vortex wake. As a consequence, the periodic hydrodynamic forces feeding back from the vortex-shedding mechanism are considerably reduced, if not completely suppressed. In theory, the mean drag acting on the body is also reduced if suppression of the vortex wake is achieved [3,1]. Therefore, the development of passive devices to control the wake of a bluff body has called the attention of not only the scientific community, but also of the industry. Applications may vary from reduction of vortex-generated noise in the field of aeroacoustics to the mitigation of hydrodynamic loads on floating platforms in the field of offshore engineering. The suppression of the flow-induced motion of offshore risers or of a monocolumn platform are good examples [15].

Placing a smaller control rod upstream of the main cylinder is also a well-established strategy for drag reduction [10]. But Strykowski and Sreenivasan [18] have proved that if the small control cylinder is placed within a defined region in the near-wake (downstream) of the main cylinder, coherent vortices could be effectively suppressed at a Reynolds number of $Re = 80$. Hwang and Choi [4] showed that the flow instability leading to the formation of a vortex street could be delayed by employing even smaller control cylinders at specific locations in the wake. Later, Kuo et al. [9] and Kuo and Chen [8] proved that, even if a vortex-wake is formed, the wake pattern could be altered by the presence of two control cylinders positioned in the near wake region.

Previous investigations positioning control cylinders in various arrangements around a bluff body have been performed through experiments and numerical simulations. Mittal [11] investigated the flow around a static cylinder with two wake-control cylinders positioned at $\pm 90^{\circ}$ in relation to the incoming flow at $Re = 10^2$ to 10^4. He found that vortex shedding could be suppressed only if the control cylinders (at that specific $\pm 90^{\circ}$ location) were rotating above a critical spinning ratio. Sakamoto and Haniu [16] also investigated the control of a vortex-wake by varying the position of a smaller cylinder around the main body. They observed that, for certain positions, the control cylinder could produce the useful

* Corresponding author.
E-mail address: g.assi@usp.br (G.R.S. Assi).
[1] Now at the Dept. Naval Architecture, Universidad Veracruzana, Mexico.
[2] Currently a Visiting Associate in Aerospace at GALCIT, California Institute of Technology, USA.

http://dx.doi.org/10.1016/j.expthermflusci.2017.03.020
0894-1777/

effect of reducing the hydrodynamic forces experienced by the main body at $Re = 6.5 \times 10^4$.

Recently, Silva-Ortega [17] has shown that a polar array of 2, 4 and 8 control cylinders equally spaced around a static body could be developed into an effective device to suppress vortex shedding from a larger circular cylinder at $Re = 5000$ to $50,000$. Fundamental parameters (such as the number of control cylinders, their diameter and their distance from the main body) have been shown to play a significant role in the wake-control mechanism. As consequence, a reduction of hydrodynamic forces has been achieved.

1.1. Suppression of flow-induced vibration

In the present work, we move from controlling the wake of static bluff bodies to the field of hydroelasticity. This time we investigate the effectiveness of a polar array of control cylinders in suppressing the vortex-induced vibrations (VIV) of a circular cylinder that is free to respond to the excitation of the incoming flow. Our investigation is limited to vibrations in one degree of freedom in the cross-flow direction.

VIV is a fluid-structure interaction phenomenon that occurs when the frequency of vortex shedding resonates with one of the natural frequencies of an elastic bluff body. Please refer to Williamson and Govardhan [19] for a comprehensive review of the phenomenon. In principle, if a device is able to suppress the formation of coherent vortices, VIV is eliminated at its root and vibrations do not develop. Now, it is one thing to disrupt or control the wake of a bluff body when the body is static, but it is another to control the wake of a body that is free to respond to the flow. Sometimes an efficient device for the control of vortex-shedding is not as efficient in suppressing VIV. Various examples of VIV suppressors are found in the literature, for example, in the review by Zdravkovich [22].

Korkischko and Meneghini [7] have performed VIV experiments with a circular cylinder free to oscillate in the cross-flow direction and fitted with two wake-control cylinders in the range of $Re = 7500$. They found that the two non-rotating control cylinders positioned at $\pm 90^\circ$ were not effective in suppressing VIV of the main body. In fact, they only reduced the peak amplitude of response by 17%, when compared to that of a plain cylinder. However, when they applied enough rotation to the small cylinders, the vortex wake was stabilized and VIV was suppressed.

Zhu et al. [23] performed numerical simulations of the flow at $Re = 2000$ and showed that the two-degree-of-freedom vibration of an elastic cylinder could be reduced by 89% when two control cylinders were positioned at $\pm 135^\circ$ from the frontal stagnation point of the cylinder. Again, when the two control cylinders were forced to rotate, an ever better suppression was obtained. Similar results were obtained by Muddada and Patnaik [13], who performed two-dimensional numerical simulations of the flow around a cylinder fitted with two control cylinders located at $\pm 120^\circ$ in the range of $Re = 100$–300.

Wu et al. [21] tested the VIV suppression of a long flexible cable with a circular cross section fitted with four flexible control rods positioned parallel to the axis of the cylinder. At $Re \approx 10^3$, they observed that the dynamic response of the cable was substantially altered by the hydrodynamic interaction of the flow-control rods. In their experimental arrangement, the distribution of the control rods was such that there was always one rod aligned with the incoming flow. In another study, Wu et al. [20] investigated the effect of rotating the array of control rods around the main cylinder.

1.2. Objective

In the present study, we start with the polar arrays of 2, 4 and 8 control cylinders proposed by Silva-Ortega [17] to reduce the hydrodynamic loads on a static cylinder and employ them as a means to suppress the cross-flow VIV of a larger elastic circular cylinder. The dynamic response due to VIV, as well has the hydrodynamic loads acting on the cylinder, are presented for a wide range of flow speeds.

We will conclude that the VIV of a circular cylinder can be mitigated by specific arrangements of wake-control cylinders in the range of Reynolds number between 5000 and 50,000. On the other hand, a few arrangements may cause the system to develop severe vibrations associated with a galloping-like excitation, showing that the dynamic response of the system is very sensitive to small variations in the geometrical parameters.

2. Experimental setup

Experiments have been carried out in the Circulating Water Channel of NDF (Fluids and Dynamics Research Group) at the University of São Paulo, Brazil. The water channel has an open test section which is 0.7 m wide, 0.9 m deep and 7.5 m long. Good quality flow can be achieved up to 1.0 m/s with turbulence intensity less than 3%. For further details on the apparatus, other VIV experiments employing the elastic rig and information on the facilities please refer to Silva-Ortega [17] or Assi et al. [2].

A rigid section of a smooth circular cylinder was made of a perspex tube of external diameter $D = 100$ mm. Two, four or eight identical wake-control cylinders of diameter d_c were made of perspex rods and supported by rings attached to the ends of the main cylinder. The distribution of the control cylinders about the main cylinder is presented in Fig. 1, in which the arrow indicates the direction of the incoming flow. The position of the N control cylinders was chosen so that they are equally spaced around the main cylinder, but keeping a symmetric distribution in relation to the streamwise axis, with no cylinder at the frontal stagnation point.

It is worth noting that our cylinder fitted with 2 control cylinder is similar to other arrangements found in the literature ([7,11] for example). Our arrangement with 4 control cylinder is not similar to that of Wu et al. [21], since they always kept one control cylinder facing the incoming flow. We are not aware of other works that have employed an array of $N = 8$ wake-control cylinders.

The axes of the control cylinders were parallel to the axis of the main cylinder, spanning the whole immersed length of the model ($L = 700$ mm). Two extra supporting rings were installed at $L/3$ and $L2/3$ positions to hold the control cylinders in place and prevent them from vibrating by reducing their free span. The control cylinders did not present significant deflections nor vibrations due to their own VIV in the course of the experiments.

Inspired by the experimental results of Korkischko and Meneghini [7] and based on the parametric variation of Silva-Ortega [17], the diameter of the control cylinders was varied in three steps of $d_c/D = 0.04$, 0.06 and 0.08. The gap measured between the wall of the control cylinders and the wall of the main cylinder was set to $G/D = 0.05$, 0.10 and 0.15. A total of 27 geometric variations employing the wake-control cylinder have been tested, in addition to the case of a plain cylinder (without control cylinders) that served a reference.

Models were mounted on a especially built load cell attached to a sliding frame and supported by air bearings. A pair of coil springs provided the restoration force to the system, which was free to oscillate only in the cross-flow direction, as shown in Fig. 2. An optical sensor measured the displacement (y) of the cylinder, keeping structural mass and damping to a minimum. The product between the mass ratio (m^*, calculated as the ratio between the total oscillating mass and the mass of displaced water) and the damping ratio (ζ, measured as a percentage of the critical damping) was $m^*\zeta = 0.066$. The natural frequency of the system (f_0) as well

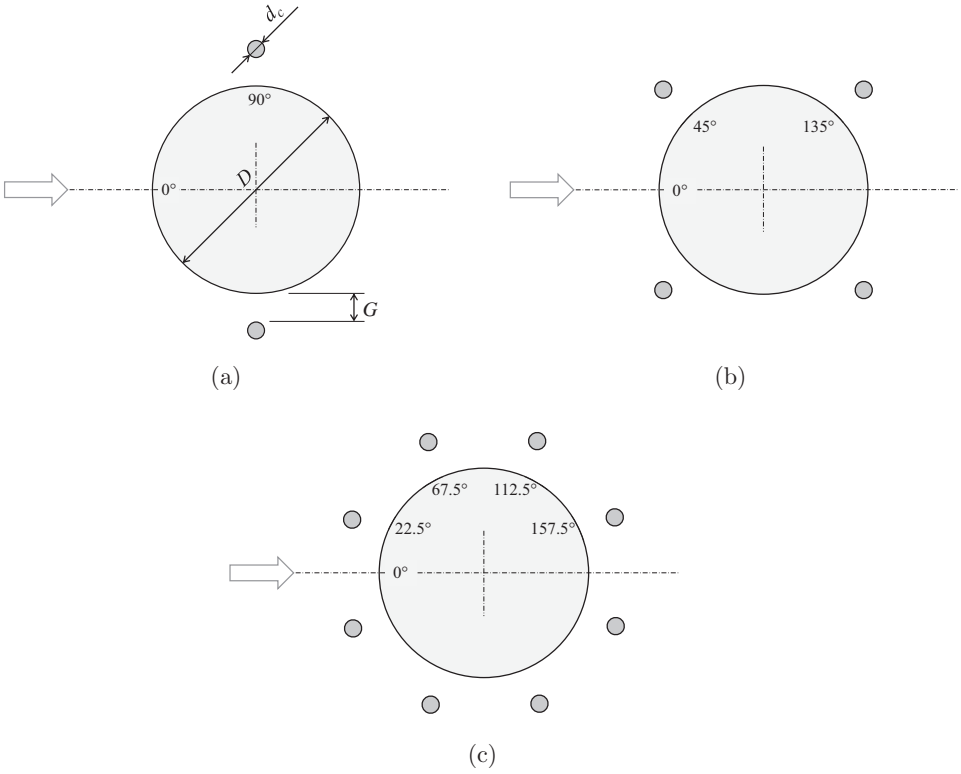

Fig. 1. Geometrical parameters for the main cylinder with (a) two, (b) four and (c) eight control cylinders (figures drawn not to scale). Incoming flow direction marked by the arrow.

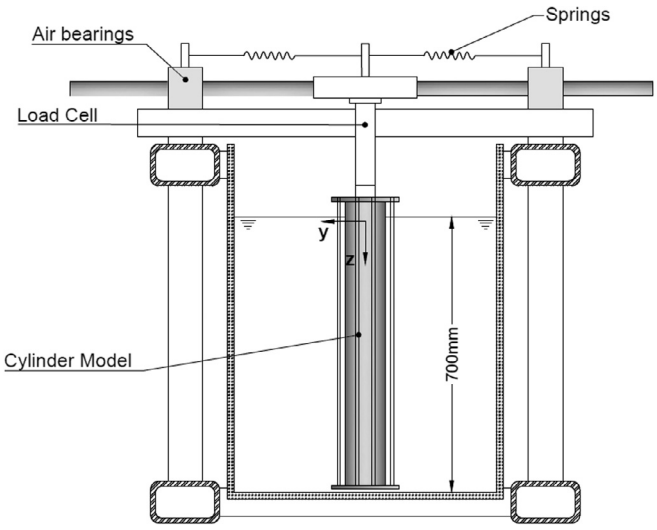

Fig. 2. Cross view of the experimental setup: elastic rig mounted on the test section.

as the damping ratio (ζ) were determined by decay tests performed in air.

The only flow variable changed during the course of the experiments was the flow speed (U), which altered $Re = UD/\nu$ between 5000 and 50,000 (where ν is the dynamic viscosity of water) and the reduced velocity $U_R = U/(Df_0)$ in the range of 2 to 20. A summary of all the parameters investigated in the experiment is presented in Table 1.

The dynamic responses due to VIV are analyzed across the U_R range by comparing the normalized amplitude of displacement $\hat{y}/D$, where $\hat{y}$ is the RMS of y times $\sqrt{2}$ (also called harmonic amplitude). The dominant frequency of oscillation normalized by the natural frequency (f/f_0) was obtained from the spectrum of displacement with a non-dimensional resolution of 0.02. The mean drag coefficient ($\overline{C}_D$) and the RMS of the lift coefficient ($\widehat{C}_L$) were obtained by reducing the force measurement of the load cell with the product $\frac{1}{2}\rho U^2 D$, per unit length of the cylinder (where ρ is the specific mass of the water). The experimental uncertainties for the measurements of all variables and parameters are specified in Table 1.

3. Results and discussion

Preliminary VIV results were obtained for a plain cylinder to validate the setup and serve as reference for comparison. Fig. 3a presents the amplitude of displacement ($\hat{y}/D$) compared to the results of Khalak and Williamson [6], who performed VIV experiments with low damping at $m^* = 2.4$ and 3.3. The peak amplitude of response is almost $\hat{y}/D = 1$ around $U_R = 4$ and the typical three branches of response (initial, upper and lower) are clearly identified in both datasets. The wider synchronization range observed in the present data, extending from $U_R = 3$ to almost 15, is due to our lower value of $m^* = 1.09$.

While Khalak and Williamson [6] normalized U_R employing the natural frequency of the system immersed in still water (f_N, in their notation), their previous work [5] had presented the same data non-dimensionalizing U_R by the natural frequency measured in air (f_0). In the present paper we have recalculated the U_R axis from Khalak and Williamson [6] based on their data presented in 1996 to allow for a direct comparison of the data. Even though there are small differences in m^* and ζ, the agreement is very good.

Fig. 3b shows the dominant frequency of vibration (f/f_0). The inclined line represents a nominal Strouhal number $St = 0.2$, which

Table 1
Parameters and variables employed in the present investigation.

Parameter or Variable	Symbol	Variation	Uncertainty (%)
Number of control cylinders	N	0, 2, 4, 8	
Diameter of control cylinders	d_c/D	0.04, 0.06, 0.08	±5
Gap between cylinders	G/D	0.05, 0.10, 0.15	±5
Reynolds number	Re	5×10^3–5×10^4	±5
Reduced velocity	U_R	2–20	±5
Mass ratio	m^*	1.09	±5
Damping ratio	ζ	0.0061	±7
Harmonic amplitude of displacement	$\hat{y}/D$		±3
Dominant frequency of oscillation	f/f_0		±5
Mean drag coefficient	$\overline{C}_D$		±3
RMS of lift coefficient	$\widehat{C}_L$		±5

is expected for a plain, static cylinder in this Re range. Both curves show the synchronization range within which the frequency of vortex-shedding is locked by the frequency of oscillation (f). The curves depart from the $St = 0.2$ line and follow closer to $f/f_0 = 1$. Even though the present data only shows the dominant frequencies of response – and not concurrent frequency branches along the U_R range – the overall trend is in agreement with the reference.

Fig. 3c shows the mean drag ($\overline{C}_D$) as a function of U_R, revealing the amplification of drag during the synchronization range. The maximum $\overline{C}_D \approx 4$ is consistent in both curves. The fluctuating lift coefficients, presented in Fig. 3d, also show good agreement with the results of Khalak and Williamson [6]. Even though our results show a local amplification of $\widehat{C}_L$ between $U_R = 7$ and 10, corresponding to the transition from the upper to the lower branch of response, the maximum values of $\widehat{C}_L \approx 2.5$ are in very good agreement.

3.1. VIV response with 2 control cylinders

Fig. 4a presents the VIV response for the case with 2 control cylinders compared with that of a plain cylinder. In general, all cases with 2 control cylinders presented peak amplitudes of vibration at resonance ($U_R \approx 4$) lower than that experienced by the plain cylinder. But while the end of the VIV synchronization range was clearly noticeable for the plain cylinder at $U_R = 15$, all systems with 2 control cylinders sustained greater $\hat{y}/D$ for the higher reduced velocities.

The results obtained by Korkischko and Meneghini [7] for a system with two control cylinders are also presented in Fig. 4a for comparison. In their experiment, Re was varied between 1600 and 7500 and the geometrical parameters were $[d_c/D, G/D] = [0.06, 0.07]$, which fits in between our two cases with $[d_c/D, G/D] = [0.06, 0.05]$ and $[0.06, 0.10]$. Their response curve revealed a single branch of considerable vibration extending until the end of the U_R range. While their maximum $\hat{y}/D \approx 0.6$ was not too far from our results (which showed $\hat{y}/D \approx 0.7$), their system did not develop severe vibrations for the higher reduced velocities. On the other hand, our results showed a considerable build-up of response with increasing flow speeds, with $[d_c/D, G/D] = [0.06, 0.10]$ reaching $\hat{y}/D \approx 1.3$ at $U_R = 17$. Korkischko and Meneghini [7] concluded that their system did not respond due to a galloping instability even though their control cylinders broke the axial-symmetry of the body, making it, at least in theory, susceptible to galloping.

This fundamental difference in the responses may suggest that Re could play an important role in the dynamics of the system. The difference of Re between the two experiments was only of one order of magnitude, but it might have been that different regimes of separated flow could have sustained galloping-like oscillations for higher reduced velocities in our case. Another possible explanation – and perhaps a more probable one – regards the difference in the level of structural damping of both systems. Since Korkischko and Meneghini [7] reported a $\zeta = 0.01$ (one order of magnitude higher than in the present work), it might be that the responses from both experiments are due to the same hydrodynamic mechanisms, but balancing different levels of structural damping.

In general, the behavior of the cases with 2 control cylinders could be divided into two groups. The difference might not be noticeable from the $\hat{y}/D$ alone, but requires a close look in the frequency signatures presented in Fig. 4b. Three cases made a group of distinct response showing f/f_0 following closer the $St = 0.2$ line as U_R was increased. They were $[d_c/D, G/D] = [0.04, 0.15]$, [0.06, 0.15] and [0.08, 0.05]. They did not show the highest $\hat{y}/D$, but their frequency signature was rather distinct from the other cases. Somehow, the size and position of the two control cylinders made the system increase f/f_0 with U_R following the frequency of vortex shedding. As a result, considerable vibration with $\hat{y}/D \approx 0.4$ to 0.7 were sustained for higher reduced velocities at a clearly distinct frequency trend. On top of that, one has to bear in mind that such a low-$m^*\zeta$ system may also present a non-negligible residual vibration due to turbulence buffeting, especially for high flow speeds.

All other cases, apart form the three identified above, showed considerable $\hat{y}/D$ (which increases with U_R), but with a periodic response at a much lower f/f_0 signature, most of the time lower than $f/f_0 = 1$. Also, sudden jumps between different levels of dominant f/f_0 suggest a broader spectrum of vibration, with not a single branch of f/f_0 dominating over the U_R range. For some cases, f/f_0 was so low that it might indicate a slow lateral drift of the cylinder.

We believe that the build-up of $\hat{y}/D$ with increasing U_R combined with a low frequency signature suggests a galloping-like excitation. The most significant cases were $[d_c/D, G/D] = [0.06, 0.10]$, $[0.08, 0.10]$ and $[0.08, 0.15]$. Of course a detailed analysis of the lift signal would be necessary to identify the phenomenon (what is beyond the scope of this paper). Nevertheless, inspired by the classical galloping theory presented by Parkinson [14], it might be that different combinations of d_c/D and G/D for 2 control cylinders produced different amounts of lift in phase with the transverse velocity of the body to overcome the actual level of ζ. In a future investigation, visualization of the flow around the control cylinders will be required to determine if flow regimes of a different nature were in action.

Turning now to Fig. 4c, $\overline{C}_D$ curves show that all cases with 2 control cylinders presented the amplification of mean drag during and beyond the VIV synchronization range, with $\overline{C}_D$ remaining higher than that measured for the plain cylinder for higher U_R. Interestingly, the cases with the highest $\hat{y}/D$ for the higher U_R were not the ones that presented the highest $\overline{C}_D$. On the contrary, the three cases mentioned above (following the vortex-shedding frequency) presented the lowest mean drag for the widest range of U_R. The highest $\overline{C}_D$ were found for $[d_c/D, G/D] = [0.08, 0.05]$ and the other two cases governed by that distinct mechanism.

Finally, Fig. 4d does not reveal a distinct behavior that separates the cases with 2 control cylinders. Perhaps the only thing to highlight is that the highest $\widehat{C}_L$ were observed for those cases whose frequency signatures followed the $St = 0.2$ line for longest. When the response was tuned in the vortex-shedding frequency, the system was able to extract more energy from the flow, thus resulting in higher $\widehat{C}_L$.

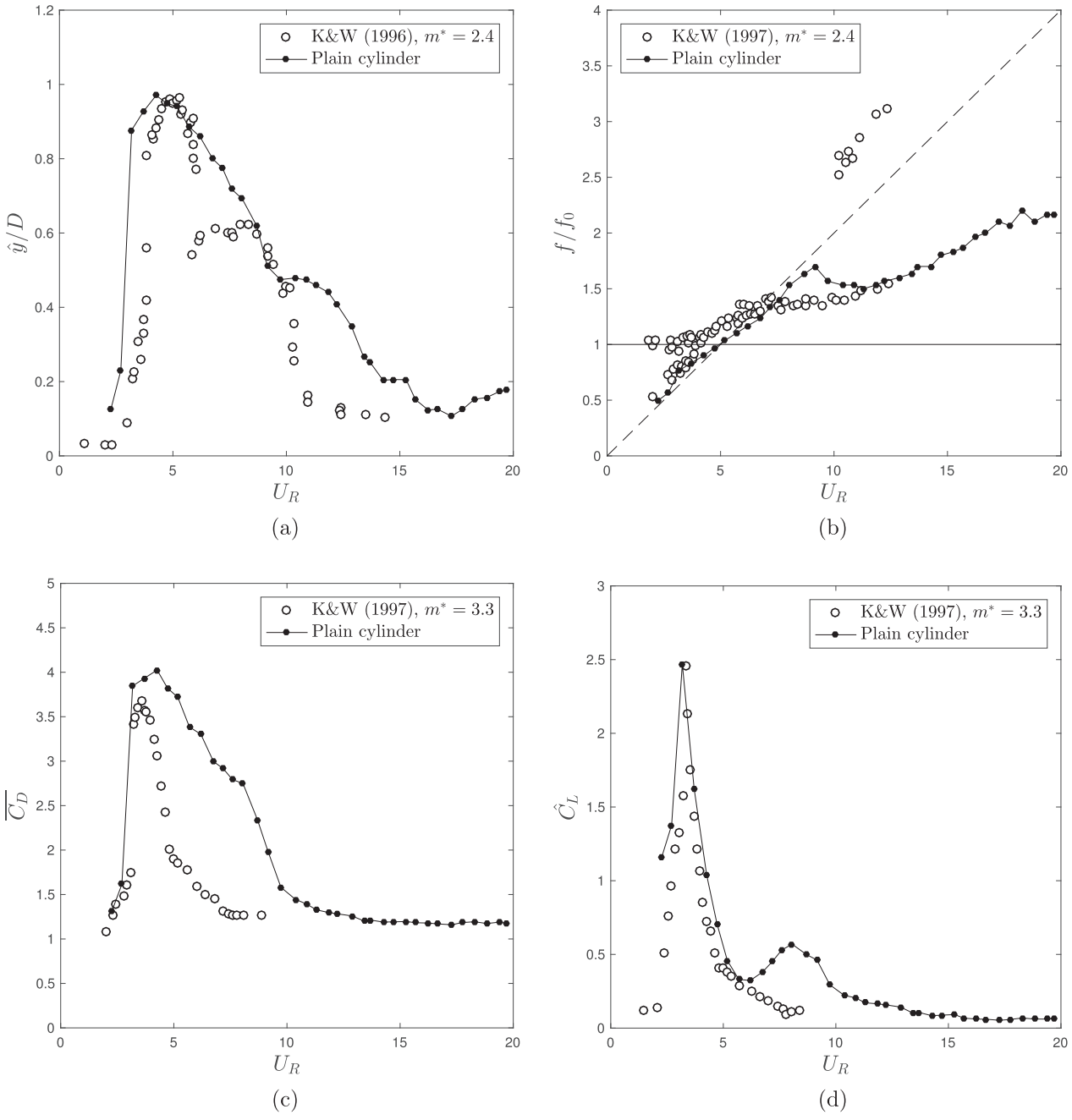

Fig. 3. Validation of the VIV response of a plain circular cylinder with $m^* = 1.09$ and $m^*\zeta = 0.066$: (a) amplitude of displacement, (b) frequency of vibration, (c) mean drag coefficient and (d) RMS of lift coefficient. Data for comparison is from Khalak and Williamson [5,6], with $m^*\zeta = 0.013$.

3.2. VIV response with 4 control cylinders

The responses are considerably different when 4 control cylinders were fitted around the main body; Fig. 5a presents $\hat{y}/D$ for all nine variations. In general, the three cases with the smallest control cylinders ($d_c/D = 0.04$) presented a reduced peak of vibration when compared to the response of the plain cylinder; $\hat{y}/D$ was also considerably reduced by the end of the synchronization range around $U_R = 14$. It appeared that these three cases were indeed responding under the influence of VIV. The best case with $[d_c/D, G/D] = [0.04, 0.05]$ reduced the peak $\hat{y}/D$ by 50%.

When d_c/D was increased to 0.06, $[d_c/D, G/D] = [0.06, 0.05]$ and $[0.06, 0.10]$ presented a suppressed response. But the clear distinct response was observed for the case $[d_c/D, G/D] = [0.06, 0.15]$, with a local resonant peak of VIV at $U_R \approx 4$, followed by a galloping-like response characterized by rapidly increasing amplitudes for $U_R > 10$. The frequency signature for $[d_c/D, G/D] = [0.06, 0.15]$, presented in Fig. 5b, showed that f/f_0 followed a clear dominant trend below 1 for the entire response. Again, it might be that a specific pair $[d_c/D, G/D]$ for 4 control cylinders was able to interact with the separated flow generating lift in phase with the transverse velocity of the body. This galloping-like mechanism is possible to occur for non-circular geometries and might have occurred for this specific case of $N = 4$ control cylinders.

The best VIV suppression for 4 control cylinders was found for $[d_c/D, G/D] = [0.08, 0.05]$, with a maximum peak of only $\hat{y}/D = 0.25$ at the VIV resonance ($U_R = 4$) and $\hat{y}/D < 0.2$ for the rest of the reduced velocity range. In contrast, the case $[d_c/D, G/D] =$

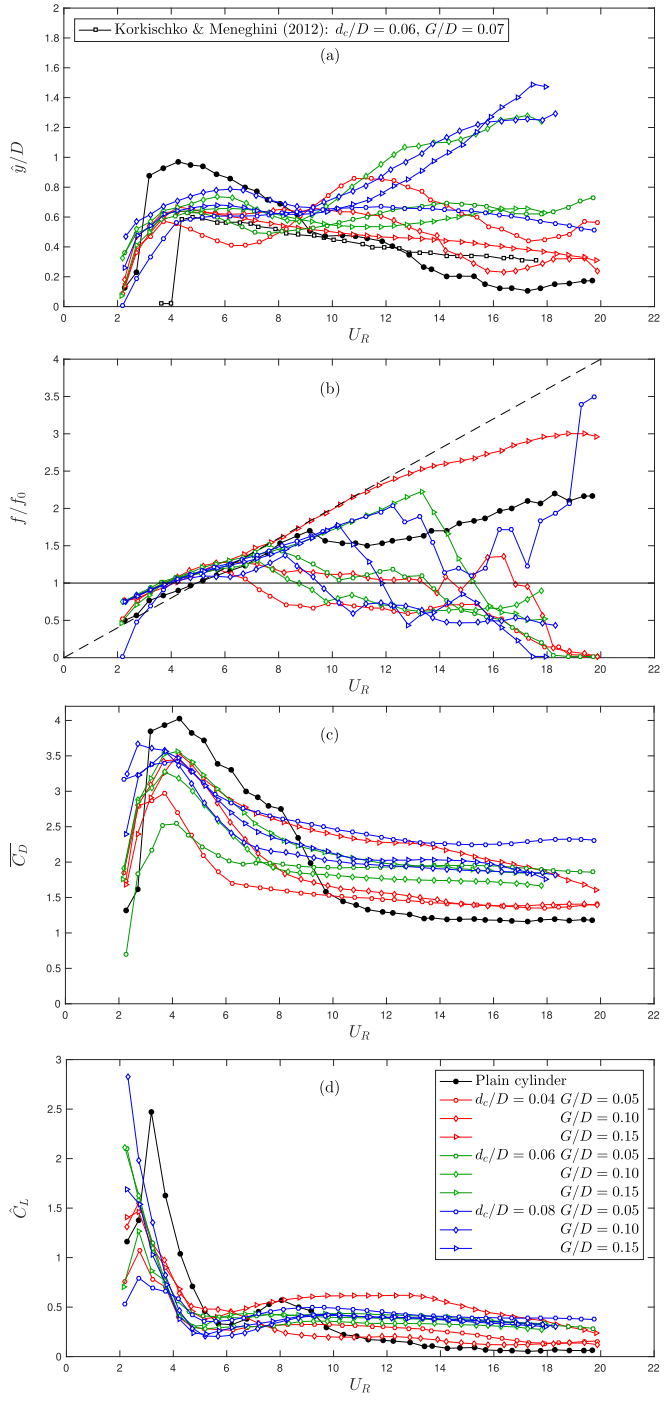

Fig. 4. VIV response for a circular cylinder with $N = 2$ control cylinders: (a) amplitude of displacement, (b) frequency of vibration, (c) mean drag coefficient and (d) RMS of lift coefficient.

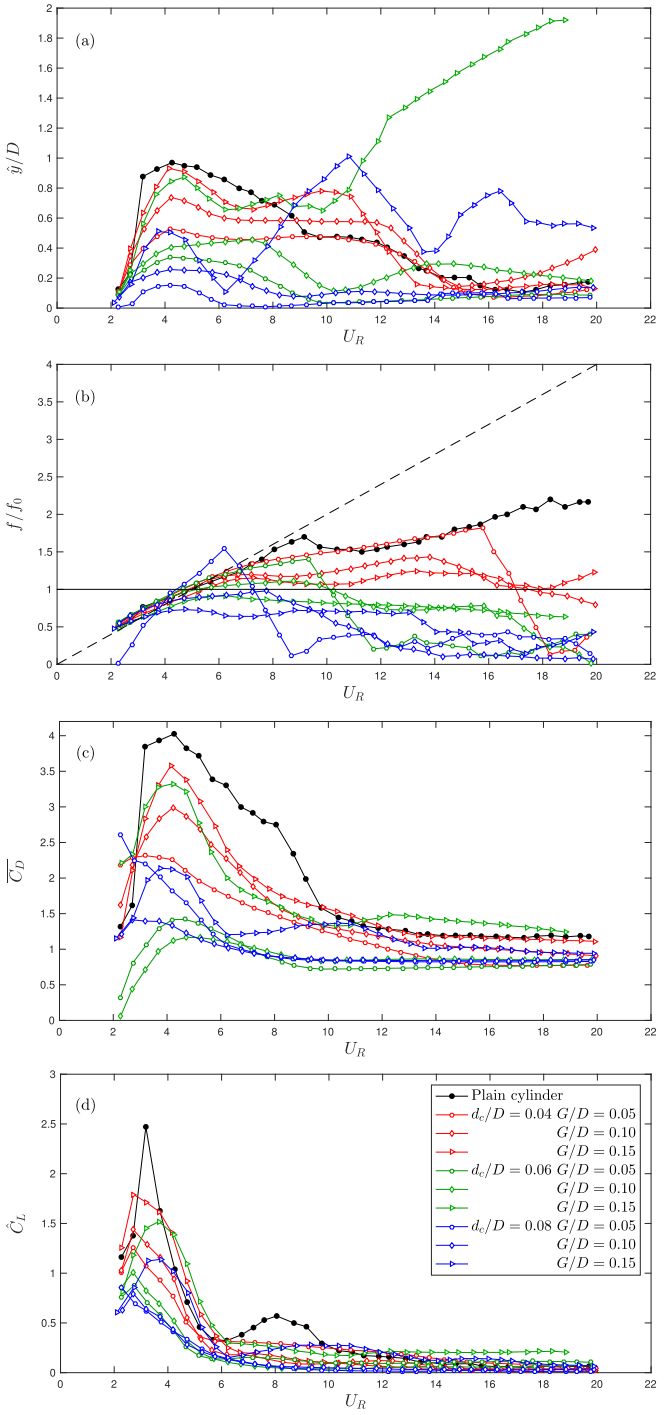

Fig. 5. VIV response for a circular cylinder with $N = 4$ control cylinders: (a) amplitude of displacement, (b) frequency of vibration, (c) mean drag coefficient and (d) RMS of lift coefficient.

$[0.08, 0.15]$ responded with a very distinct behavior, with local peaks of vibration at $U_R = 4$, 11 and 16. Its frequency signature also remained below $f/f_0 = 1$, suggesting that a galloping-like excitation was present but could not be sustained until the highest reduced velocity.

It is interesting to note in Fig. 5c that almost all cases presented $\overline{C}_D$ below that for a plain cylinder. Case $[d_c/D, G/D] = [0.06, 0.05]$, which presented a good suppression, achieved the lowest mean drag for most of the reduced velocity range. As expected, the case $[d_c/D, G/D] = [0.06, 0.15]$, with the highest response, also presented the highest $\overline{C}_D$.

3.3. VIV response with 8 control cylinders

First of all, no galloping-like responses were observed for the systems with 8 control cylinders, as seen in Fig. 6a, probably because the apparent axial-symmetry of the body is somewhat recovered with the distribution of more control cylinders. Almost all cases presented $\hat{y/D}$ under the response curve of the plain cylinder, with only a few exceptions. Cases with $[d_c/D, G/D] = [0.04, 0.10]$ and $[0.04, 0.15]$ presented the highest responses, with $\hat{y}/D \approx 0.4$ being sustained for higher U_R beyond

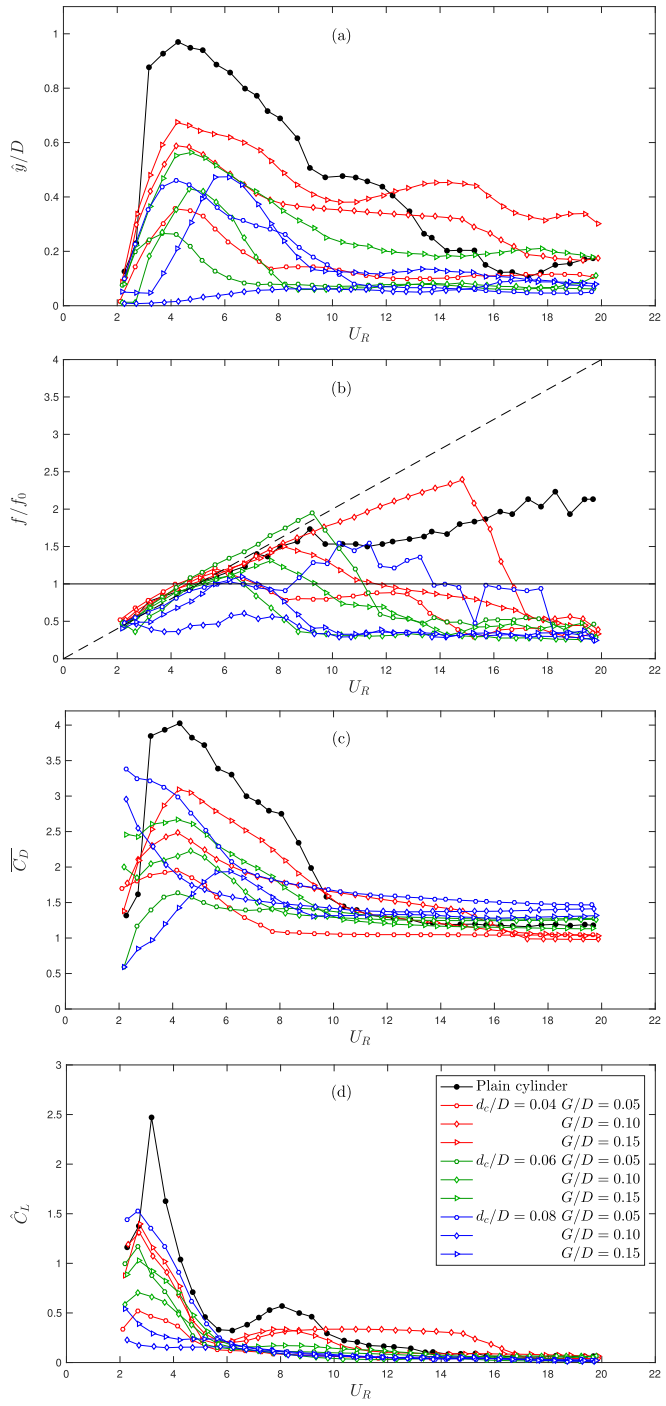

Fig. 6. VIV response for a circular cylinder with $N = 8$ control cylinders: (a) amplitude of displacement, (b) frequency of vibration, (c) mean drag coefficient and (d) RMS of lift coefficient.

the synchronization range of the plain cylinder. The frequency signatures for these two cases, shown in Fig. 6b, remained below $f/f_0 = 1$, suggesting that a mechanism other than VIV was driving the vibrations.

The best suppression was achieved by the largest control cylinders, in special by the case $[d_c/D, G/D] = [0.08, 0.10]$, that showed almost no response (in fact, a reduction by 99%) near the VIV resonance and minimum $\hat{y}/D < 0.1$ for the wider range of U_R. This case, however, did not present the lowest mean drag, which was increased by 12% when compared to that of a plain cylinder. The lowest mean drag of all was recorded for the case $[d_c/D, G/D] = [0.04, 0.05]$, as seen in Fig. 6c. Very few cases with 8 control cylinders managed to reduced the mean drag below that of the plain cylinder for the wide range of U_R. Finally, the highest $\widehat{C}_L$ was achieved by $[d_c/D, G/D] = [0.04, 0.10]$, apparently responding with f/f_0 following the frequency of vortex-shedding, as seen in Fig. 6d.

4. Further discussion

As seen above, the responses showed a variety of different behaviors, making it a rather difficult task to find a general governing principle with the parameters we had in hand. Sometimes, a small variation in one of the parameters produced a totally different response. In an attempt to find a general geometric parameter governing the response behavior, one could propose to add the diameter of the control cylinder to the gap between the walls, thus creating $(G + d_c)/D$. This new parameter simply represents the outermost radial distance of the control cylinders from the wall of the main cylinder, in a way suggesting how far into the flow the control cylinders could interfere.

Table 2 presents the parameter $(G + d_c)/D$ calculated for the nine parametric variations for each N control cylinders. One can easily note that $(G + d_c)/D$ more than doubles from the first to the last case. Also, one could expect that small variations in this parameter, say from $(G + d_c)/D = 0.13$ to 0.14, would not produce qualitatively different responses. Indeed, cases $[d_c/D, G/D] = [0.08, 0.05]$ and $[0.04, 0.10]$ showed qualitatively similar responses for $N = 2$ and 4, but significantly different responses for $N = 8$. In summary, simply considering the outermost position of the control cylinders represented by $(G + d_c)/D$ would not explain the complex hydrodynamic interference by grouping together similar response curves.

The most interesting general aspect is that all cases reduced maximum amplitude of vibration at the VIV resonance. Most of the cases also reduced $\hat{y}/D$ for most of the synchronization range ($3 < U_R < 13$). On the other hand, the behavior for higher reduced velocities, way past the synchronization range, appeared to have shown a complex phenomenology. Pure VIV, pure galloping-like and combined VIV and galloping-like excitations all appeared in the responses for higher values of U_R. The configurations with $N = 4$ control cylinders, for example presented the most diverse response for the set of parameters investigated (Fig. 5). At the same time that they presented the lowest recorded mean drag, they also produced the highest amplitudes of vibration with the richest frequency signatures. A small variation on the radial position and size of the control cylinders produced unexpected responses.

The group with $N = 2$ control cylinders have shown even higher levels of mean drag, the highest recorded in the investigation. Apart from the suppression of $\hat{y}/D$ within the synchronization range, all cases produced responses higher than that of the plain cylinder for $U_R > 8$. This behavior can be associated with a galloping-like excitation, especially if the frequency signature is taken into account. Korkischko and Meneghini [7] performed experiments with a similar case with 2 control cylinders with $[d_c/D, G/D] = [0.06, 0.07]$ and $m^* = 1.8$. They reported that the amplitude of response was completely different when compared to that of a plain cylinder. In fact, their peak response of

Table 2
Parameter $(G + d_c)/D$.

	$d_c/D = 0.04$	$d_c/D = 0.06$	$d_c/D = 0.08$
$G/D = 0.05$	0.09	0.11	0.13
$G/D = 0.10$	0.14	0.16	0.18
$G/D = 0.15$	0.19	0.21	0.23

$\hat{y}/D \approx 0.6$ at $U_R = 4$ was similar to our case $[0.04, 0.15]$, for which the peak amplitude was $\hat{y}/D \approx 0.7$.

Four of our cases presented galloping-like instability: three cases for $N = 2$ ($[d_c/D, G/D] = [0.08, 0.10], [0.08, 0.15]$ and $[0.06, 0.10]$); and one for $N = 4$ ($[d_c/D, G/D] = [0.06, 0.15]$). Based on the theory for classical galloping summarized by Parkinson [14], the position of the fixed control cylinders may have interacted with the separation points as the cylinders oscillated across the flow. The arrangement may have broken the body's axial-symmetry, generating lift in phase with the body's transverse velocity. Consequently, as we have observed, the amplitude of response presented a rapid increase for increasing flow speeds, with no sign of decrease, at least not in the range of the experiments.

For other cases, it appears that the high amplitudes of oscillations due to galloping are competing with or being disrupted by the resonant vibrations of VIV. This might be happening for the case with $N = 4$ and $[d_c/D, G/D] = [0.08, 0.15]$, in which galloping and VIV appear to interchangeably occur along the reduced velocity range. The peak displacement initially achieved by VIV around $U_R \approx 4$ could produce fast-enough vibrations to lead the system into galloping for the rest of the U_R range.

When the cylinder was surrounded by $N = 8$ control cylinders, no galloping-like response was observed. Apparently, the evenly distribution of more control cylinder around the body helped it to restore its axial-symmetry, at least as far as the main flow structures are concerned. One should note that galloping is highly dependent on Reynolds number, free stream turbulence intensity and other secondary factors, therefore we cannot assert that a cylinder fitted with 8 control cylinders will never develop galloping under other flow circumstances. Zdravkovich [22] presented results of a cylinder fitted with an axial-rod shroud. Several parameters were varied in order to find an optimum configuration, such as the shroud diameter and porosity. The most effective shroud geometry had $d_c/D = 1.25$ with a 63% porosity, hence this configuration was chosen to verify the optimal circumferential distribution by pulling out the rods. When the body was left with only 11 rods on each size (distributed around $\pm 90^\circ$), the amplitude of oscillation was higher than that of a plain cylinder and resembled galloping. Our results, together with Zdravkovich [22], confirm that galloping-like excitation will be very sensitive to the position of the control cylinders (especially if they are located near the separation points), therefore hydrodynamic axial-symmetry must be pursued.

5. Conclusion

Amplitude of displacement, frequency of oscillations, mean drag and fluctuating lift coefficients have been measured for a cylinder surrounded by a polar array of $N = 2$, 4 and 8 wake-control cylinders intended to act as VIV suppressors. The response showed that while some configurations suppressed the flow-induced oscillations, others enhanced them under a galloping-like mechanism.

Most of the configurations presented a VIV resonant response with a reduced amplitude of displacement when compared with that of a plain cylinder. The best case for response reduction was the configuration of 8 control cylinders with $[d_c/D, G/D] = [0.08, 0.10]$, which reduced about 99% of the peak amplitude for the whole range of reduced velocities. Consequently, mean drag was increased by 12% above the reference value for a plain cylinder beyond the synchronization range.

In a very brief summary: (i) A polar array of 8 control cylinders may achieve complete suppression of VIV without leading the system into galloping. Suppression is achieved at the cost of increasing the mean drag. (ii) A polar array of 4 control cylinders may be the most efficient configuration to minimize the mean drag, but the system may develop severe vibrations combining VIV and galloping. (iii) The system is very sensitive to the parameters investigated ($N, d_c/D$ and G/D), therefore small geometric variations in the control cylinders may produce unexpected responses.

It is worth noting that the system approximates an omnidirectional device as the number of equally-spaced control cylinders is increased. In the limit, we should be able to recover the behavior of a cylinder fitted with shrouds (or axial rods) with equivalent density. In the present investigation, the arrangement with 8 control cylinders is the closest to an axial-symmetric system. Perhaps this is the reason why the device did not develop a galloping-like instability. An omnidirectional device would be very interesting for practical applications in engineering, since the response would be independent of the incoming flow direction.

Future research should focus on the hydrodynamic mechanisms that govern the response of the system to flow-induced vibrations. Visualization of the flow in the near wake and around the control cylinders should shed light on the flow regimes that produce the distinct responses observed above. The present investigation also paves the way for experiments with active-control devices, for example, with rotating (for example, as discussed by Modi [12]) or vibrating wake-control cylinders.

Acknowledgments

MSO is grateful to CAPES Brazilian Ministry of Education. GRSA acknowledges the support of FAPESP (2011/00205-6, 2014/50279-4), CNPq (306917/2015-7) and the Brazilian Navy.

References

[1] G. Assi, P. Bearman, N. Kitney, Low drag solutions for suppressing vortex-induced vibration of circular cylinders, J. Fluids Struct. 25 (2009) 666–675.
[2] G.R.S. Assi, P.W. Bearman, B.S. Carmo, J.R. Meneghini, S.J. Sherwin, R.H.J. Willden, The role of wake stiffness on the wake-induced vibration of the downstream cylinder of a tandem pair, J. Fluid Mech. 718 (2013) 210–245.
[3] P.W. Bearman, Vortex shedding from oscillating bluff bodies, Ann. Rev. Fluid Mech. 16 (1984) 195–222.
[4] Y. Hwang, H. Choi, Control of absolute instability by basic-flow modification in a parallel wake at low Reynolds number, J. Fluid Mech. 560 (Aug) (2006) 465–-475.
[5] A. Khalak, C.H.K. Williamson, Dynamics of a hydroelastic cylinder with very low mass and damping, J. Fluids Struct. 10 (1996) 455–472.
[6] A. Khalak, C.H.K. Williamson, Fluid forces and dynamic of a hydroelastic structure with very low mass and damping, J. Fluids Struct. 11 (8) (1997) 973–982.
[7] I. Korkischko, J.R. Meneghini, Suppression of vortex-induced vibration using moving surface boundary-layer control, J. Fluids Struct. 34 (2012) 259–270.
[8] C.-H. Kuo, C.-C. Chen, Passive control of wake flow by two small control cylinders at reynolds number 80, J. Fluids Struct. 25 (6) (2009) 1021–1028.
[9] C.-H. Kuo, L.-C. Chiou, C.-C. Chen, Wake flow pattern modified by small control cylinders at low Reynolds number, J. Fluids Struct. 23 (2007) 938–956.
[10] S.-J. Lee, S.-I. Lee, C.-W. Park, Reducing the drag on a circular cylinder by upstream installation of a small control rod, Fluid Dynam. Res. 34 (4) (2004) 233–250.
[11] S. Mittal, Control of flow past bluff bodies using rotating control cylinders, J. Fluids Struct. 15 (2) (2001) 291–326.
[12] V. Modi, Moving surface boundary-layer control: a review, J. Fluids Struct. 11 (6) (1997) 627–663.
[13] S. Muddada, B. Patnaik, An active flow control strategy for the suppression of vortex structures behind a circular cylinder, Eur. J. Mech.-B/Fluids 29 (2) (2010) 93–104.
[14] G. Parkinson, Phenomena and modelling of flow-induced vibrations of bluff bodies, Prog. Aerospace Sci. 26 (2) (1989) 169–224.
[15] L.V.S. Sagrilo, M.Q. Siqueira, T.A.G. Lacerda, G.B. Ellwanger, E.C.P. Lima, E.F.N. Siqueira, VIM and wave-frequency fatigue damage analysis for SCRs connected to monocolumn platforms, in: ASME 2009 28th International Conference on Ocean, Offshore and Arctic Engineering. No. OMAE2009-79807, 2009, pp. 723–729.
[16] H. Sakamoto, H. Haniu, Optimum suppression of fluid forces acting on a circular cylinder, J. Fluids Eng. 116 (2) (1994) 221–227.
[17] M. Silva-Ortega, Suppression of vortex-induced vibration of a circular cylinder with fixed and rotating control cylinders Master's thesis, University of São Paulo, 2015, <www.teses.usp.br>.

[18] P.J. Strykowski, K.R. Sreenivasan, On the formation and suppression of vortex shedding at low Reynolds numbers, J. Fluid Mech. 218 (1990) 71–107.
[19] C.H.K. Williamson, R. Govardhan, Vortex-induced vibrations, Ann. Rev. Fluid Mech. 36 (2004) 413–455.
[20] H. Wu, D. Sun, L. Lu, B. Teng, G. Tang, J. Song, Influence of attack angle on viv suppression by multiple control rods for long flexible riser model, in: Proceedings of the 21st International Offshore and Polar Engineering Conference, 2011, p. 1276.
[21] H. Wu, D. Sun, L. Lu, B. Teng, G. Tang, J. Song, Experimental investigation on the suppression of vortex-induced vibration of long flexible riser by multiple control rods, J. Fluids Struct. 30 (2012) 115–132.
[22] M. Zdravkovich, Review and classification of various aerodynamic and hydrodynamic means for suppressing vortex shedding, J. Wind Eng. Indust. Aerodynam. 7 (1981) 145–189.
[23] H. Zhu, J. Yao, Y. Ma, H. Zhao, Y. Tang, Simultaneous {CFD} evaluation of {VIV} suppression using smaller control cylinders, J. Fluids Struct. 57 (2015) 66–80.